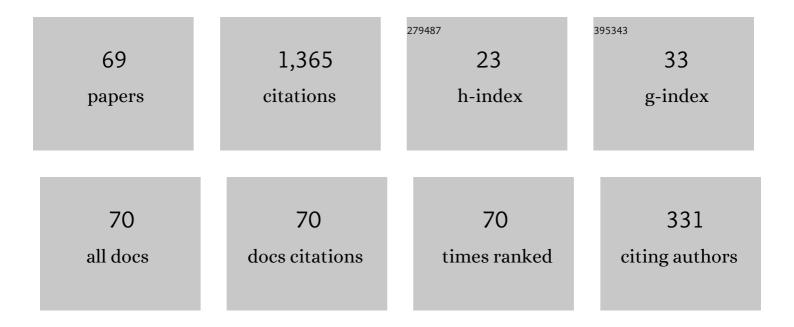
## Huazhi Gu

List of Publications by Year in descending order

Source: https://exaly.com/author-pdf/7101717/publications.pdf Version: 2024-02-01



Нилтні Сц

#	Article	IF	CITATIONS
1	Possible improvements of alumina–magnesia castable by lightweight microporous aggregates. Ceramics International, 2015, 41, 1263-1270.	2.3	86
2	Slag Resistance Mechanism of Lightweight Microporous Corundum Aggregate. Journal of the American Ceramic Society, 2015, 98, 1658-1663.	1.9	68
3	Isolation or corrosion of microporous alumina in contact with various CaO-Al 2 O 3 -SiO 2 slags. Corrosion Science, 2017, 120, 211-218.	3.0	55
4	Corrosion of Al2O3–Cr2O3 refractory lining for high-temperature solid waste incinerator. Ceramics International, 2015, 41, 14748-14753.	2.3	50
5	Properties and microstructures of lightweight alumina containing different types of nano-alumina. Ceramics International, 2018, 44, 17885-17894.	2.3	48
6	Slag corrosion-resistance mechanism of lightweight magnesia-based refractories under a static magnetic field. Corrosion Science, 2020, 167, 108517.	3.0	46
7	Correlations among processing parameters and porosity of a lightweight alumina. Ceramics International, 2018, 44, 14076-14081.	2.3	45
8	Dynamic interaction of refractory and molten steel: Corrosion mechanism of alumina-magnesia castables. Ceramics International, 2018, 44, 14617-14624.	2.3	45
9	Effect of nano-alumina sol on the sintering properties and microstructure of microporous corundum. Materials and Design, 2016, 89, 21-26.	3.3	40
10	Design, fabrication and properties of lightweight wear lining refractories: A review. Journal of the European Ceramic Society, 2022, 42, 744-763.	2.8	38
11	Effects of MgO micropowder on microstructure and resistance coefficient of Al2O3–MgO castable matrix. Ceramics International, 2014, 40, 7023-7028.	2.3	33
12	Al–Si @ Al2O3 @ mullite microcapsules for thermal energy storage: Preparation and thermal properties. Solar Energy Materials and Solar Cells, 2020, 217, 110697.	3.0	33
13	Enhanced corrosion resistance through the introduction of fine pores: Role of nano-sized intracrystalline pores. Corrosion Science, 2019, 161, 108182.	3.0	32
14	Effects of aggregate microstructure on slag resistance of lightweight Al2O3-MgO castable. Ceramics International, 2017, 43, 16495-16501.	2.3	31
15	Corrosion modeling of magnesia aggregates in contact with CaO–MgO–SiO <sub>2</sub> slags. Journal of the American Ceramic Society, 2020, 103, 2128-2136.	1.9	31
16	Mathematical Modeling on Erosion Characteristics of Refining Ladle Lining with Application of Purging Plug. Metallurgical and Materials Transactions B: Process Metallurgy and Materials Processing Science, 2013, 44, 744-749.	1.0	30
17	Fabrication and analysis of lightweight magnesia based aggregates containing nano-sized intracrystalline pores. Materials and Design, 2020, 186, 108326.	3.3	30
18	Fabrication and properties of in situ intergranular CaZrO3 modified microporous magnesia aggregates. Ceramics International, 2020, 46, 16956-16965.	2.3	28

Ниагні Gu

#	Article	IF	CITATIONS
19	Effect of MgO micropowder on sintering properties and microstructures of microporous corundum aggregates. Ceramics International, 2015, 41, 5857-5862.	2.3	27
20	Fabrication and characterization of lightweight microporous alumina with guaranteed slag resistance. Ceramics International, 2016, 42, 8724-8728.	2.3	27
21	Influence of pore distribution on the equivalent thermal conductivity of low porosity ceramic closed-cell foams. Ceramics International, 2018, 44, 19319-19329.	2.3	26
22	Corrosion mechanism of Al2O3–SiC–C refractory by SiO2–MgO-based slag. Ceramics International, 2020, 46, 28262-28267.	2.3	25
23	Characterisation and properties of low-conductivity microporous magnesia based aggregates with in-situ intergranular spinel phases. Ceramics International, 2021, 47, 11063-11071.	2.3	25
24	Slag corrosion mechanism of lightweight Al <sub>2</sub> O <sub>3</sub> –MgO castable in different atmospheric conditions. Journal of the American Ceramic Society, 2018, 101, 2096-2106.	1.9	24
25	Fabrication of lightweight alumina with nanoscale intracrystalline pores. Journal of the American Ceramic Society, 2020, 103, 2262-2271.	1.9	24
26	Effects of particle distribution of matrix on microstructure and slag resistance of lightweight Al 2 O 3 –MgO castables. Ceramics International, 2016, 42, 1964-1972.	2.3	23
27	Towards chrome-free of high-temperature solid waste gasifier through in-situ SiC whisker enhanced silica sol bonded SiC castable. Ceramics International, 2017, 43, 3330-3338.	2.3	22
28	Fabrication of CaO–MgO–Al2O3 materials from metallurgical waste industrial residue and their potential usage in MgO–C refractories. Ceramics International, 2020, 46, 959-967.	2.3	22
29	Corrosion mechanism of lightweight microporous aluminaâ€based refractory by molten steel. Journal of the American Ceramic Society, 2019, 102, 3705-3714.	1.9	21
30	Thermal properties of Al–Si/Al2O3 core–shell particles prepared by using steam hydration method. Journal of Alloys and Compounds, 2020, 817, 152801.	2.8	21
31	Towards prediction of local corrosion on alumina refractories driven by Marangoni convection. Ceramics International, 2018, 44, 1675-1680.	2.3	20
32	Research on thermal shock resistance of porous refractory material by strain-life fatigue approach. Ceramics International, 2020, 46, 14884-14893.	2.3	18
33	Improvement in fatigue resistance performance of corundum castables with addition of different size calcium hexaluminate particles. Ceramics International, 2019, 45, 225-232.	2.3	15
34	Computational Modeling and Prediction on Viscosity of Slags by Big Data Mining. Minerals (Basel,) Tj ETQq0 0 (	) rgBT/Ove	erlock 10 Tf 5
35	Enhancement of bonding network for silica sol bonded SiC castables by reactive micropowder. Ceramics International, 2017, 43, 8850-8857.	2.3	13

Incorporating Zr combined Si and C to achieve self-repairing ability and enhancement of silica sol
bonded SiC castables. Journal of Alloys and Compounds, 2018, 732, 396-405.

Ниагні Gu

#	Article	IF	CITATIONS
37	Fabrication of lightweight alumina containing fine closed pores by controlling the relationship between phase stress and superplasticity: Experimental and mathematical studies. Ceramics International, 2018, 44, 20034-20042.	2.3	13
38	Novel phenomenon of quasiâ€volcanic corrosion on the alumina refractoryâ€slagâ€air interface. Journal of the American Ceramic Society, 2020, 103, 6639-6649.	1.9	13
39	Formation Mechanism of In Situ Intergranular CaZrO3 Phases in Sintered Magnesia Refractories. Metallurgical and Materials Transactions A: Physical Metallurgy and Materials Science, 2020, 51, 5328-5338.	1.1	13
40	Improving mullite-silicon carbide refractory in coke dry quenching using aluminum nitride whiskers formed in situ. Ceramics International, 2017, 43, 16993-16999.	2.3	12
41	Effect of lightweight refractories on the cleanness of bearing steels. Ceramics International, 2018, 44, 12965-12972.	2.3	12
42	Towards chrome-free lining for plasma gasifiers using the CA6-SiC castable based on high-temperature water vapor corrosion. Ceramics International, 2019, 45, 12429-12435.	2.3	12
43	Mechanical performance and oxidation resistance of SiC castables with lamellar Ti3SiC2 coatings on SiC aggregates prepared by SPS. Journal of Alloys and Compounds, 2019, 791, 461-468.	2.8	10
44	Effect of Ti combined with Si and C on mechanical performance and oxidation resistance of SiC castables for plasma gasifier. Ceramics International, 2019, 45, 4147-4151.	2.3	10
45	Visual measurement and characterisation of quasi-volcanic corrosion at alumina ceramic-oxides melt-air interface. Journal of the European Ceramic Society, 2021, 41, 400-410.	2.8	10
46	Fabrication of in-situ Ti(C,N) phase toughened Al2O3 based ceramics from natural bauxite. Ceramics International, 2021, 47, 25497-25504.	2.3	10
47	Incorporating Zr to achieve self-protecting and enhancement of silica sol bonded SiC castables at active oxidation condition. Ceramics International, 2018, 44, 6089-6095.	2.3	9
48	Chemical interactions between a calcium aluminate glaze and molten stainless steel containing alumina inclusions. Ceramics International, 2018, 44, 1099-1103.	2.3	8
49	Role of liquid phase amounts in the pore evolution of lightweight bauxite: Experimental and thermal simulation studies. Ceramics International, 2019, 45, 6216-6222.	2.3	8
50	Corrosion resistance and antiâ€reaction mechanism of Al <sub>2</sub> O <sub>3</sub> â€based refractory ceramic under weak static magnetic field. Journal of the American Ceramic Society, 2022, 105, 2869-2877.	1.9	8
51	Pore evolution of microporous magnesia aggregates with the introduction of nano-sized MgO. Ceramics International, 2022, 48, 18513-18521.	2.3	8
52	Improvement of Durability of Purging Plugs Using MgO Micropowder for Refining Ladles. International Journal of Applied Ceramic Technology, 2016, 13, 1104-1111.	1.1	5
53	Mechanical Strength and Thermal Conductivity of Modified Expanded Vermiculite/Forsterite Composite Materials. Journal of Materials Engineering and Performance, 2016, 25, 15-19.	1.2	5
54	Effect of magnesia-calcium hexaaluminate refractories on the quality of low-carbon alloy steel. Ceramics International, 2022, 48, 31181-31190.	2.3	5

Ниагні Gu

#	Article	IF	CITATIONS
55	The Interfacial Behavior of Alumina-Magnesia Castables and Molten Slag under an Alternating Magnetic Field. InterCeram: International Ceramic Review, 2018, 67, 36-43.	0.2	4
56	Improved bonding properties of rectorite clay slurry after wet/dry grinding. Applied Clay Science, 2019, 183, 105318.	2.6	4
57	Effect of zirconia sol on the microstructure and properties of Al2O3-based ceramic fabricated from natural bauxite. Ceramics International, 2022, 48, 12954-12961.	2.3	4
58	Numerical simulation of heat transfer for Al-Si@Al2O3 composite phase change heat storage particles. Journal of Energy Storage, 2022, 52, 104953.	3.9	4
59	Microstructures and properties of in situ lamellar Al4SiC4 bonded SiC bricks: The effect of induction heating. Journal of Alloys and Compounds, 2021, 870, 159463.	2.8	3
60	Synthesis, characterization, visualization, and growth mechanism of macro-sized tubular MgO crystals formed in situ from refractory magnesia with aluminum. Ceramics International, 2022, 48, 23800-23807.	2.3	3
61	Corrosion Mechanism of Foamed Slag on the Lightweight Corundum-Spinel Castable. InterCeram: International Ceramic Review, 2016, 65, 226-231.	0.2	2
62	The Interfacial Behavior of Alumina-Magnesia Castables and Molten Slag under an Alternating Magnetic Field. InterCeram: International Ceramic Review, 2018, 67, 58-65.	0.2	2
63	Corrosion Mechanisms of Different Refractory Aggregates in Contact with SiO2-MgO-Based Slag. InterCeram: International Ceramic Review, 2020, 69, 22-29.	0.2	2
64	Bonding mechanism and performance of rectorite/ball clay bonded unfired high alumina bricks. Ceramics International, 2021, 47, 10749-10763.	2.3	2
65	Enhanced thermoelectric performance in aluminum-doped zinc oxide by porous architecture and nanoinclusions. Journal of the European Ceramic Society, 2021, 41, 3466-3472.	2.8	2
66	Improvement of low carbon MgOâ€C refractories by MAâ€CA 2 additives fabricated from metallurgical waste. International Journal of Applied Ceramic Technology, 2021, 18, 2314.	1.1	2
67	Preparation and water vapor corrosion behavior of AlN polytype bonded SiC bricks. Journal of Alloys and Compounds, 2022, , 165727.	2.8	1
68	Evolution on phase composition and properties of alumina-based ceramics fabricated from high-titania special-grade natural bauxite micropowder. Ceramics International, 2021, 47, 24574-24581.	2.3	0
69	Experiment and numerical simulation of aluminum silicon alloy corrosive treatment in the water vapor generation autoclaves. Colloids and Surfaces A: Physicochemical and Engineering Aspects, 2021, 630, 127515.	2.3	0